The Role of p38α Mitogen-Activated Protein Kinase Activation in Renal Fibrosis

COSIMO STAMBE,*† ROBERT C. ATKINS,*† GREG H. TESCH,*† TAKAO MASAKI,* GEORGE F. SCHREINER,‡ and DAVID J. NIKOLIC-PATERSON*†

**Department of Nephrology and †Monash University Department of Medicine, Monash Medical Centre, Clayton, Victoria, Australia; and ‡Scios Inc., San Francisco, California.*

Abstract. The p38 mitogen-activated protein kinase (MAPK) pathway transduces external stress stimuli and is important in extracellular matrix synthesis in cell types *in vitro*; however, its role in renal fibrosis is not known. Explored was the role the p38 MAPK pathway in rat unilateral ureteric obstruction (UUO), a model of renal fibrosis induced by a noninflammatory surgical insult. In a time-course study, a marked increase in phosphorylation (activation) of p38 in both interstitial myofibroblasts and tubules was shown. Rats were then treated daily with a specific inhibitor of p38α, NPC 31169, from the time of UUO surgery until being killed 7 d later. Compared with vehicle, NPC 31169–treated rats had a significant reduction in renal fibrosis assessed by interstitial volume, collagen IV deposition, and mRNA levels. This was primarily due to a reduction in the accumulation of interstitial myofibroblasts, as shown by a reduction in the area of immunostaining for alpha–smooth muscle actin and heat shock protein 47. The increase in renal TGF-β1 mRNA and protein levels in UUO was unaltered with NPC 31169 treatment; however, connective tissue growth factor mRNA was reduced. These results demonstrate that p38α MAPK plays an important role in renal fibrosis, acting downstream of TGF-β1. Blockade of p38 MAPK reduces extracellular matrix production and may be considered a potential therapeutic option in the treatment of renal fibrosis.

Irrespective of the nature of the initial insult, renal fibrosis is considered to be the common final pathway by which kidney disease progresses to end-stage renal failure. The p38 mitogen-activated protein kinase (MAPK) pathway is an important intracellular signal transduction pathway involved in the production of proinflammatory and profibrotic mediators. However, its role in the promotion of fibrosis *in vivo*, independent of its proinflammatory function, has not been described.

The p38 MAPK pathway is activated by multiple stimuli, including IL-1, TNF-α, lipopolysaccharide, ultraviolet light, and TGF-β1. Activation results in sequential phosphorylation and activation of a series of upstream kinases, resulting in phosphorylation and activation of p38 MAPK (1–3). Currently, four isoforms of p38 are described, α, β, γ and δ, which share a degree of amino acid sequence homology but differ in cell and tissue distribution (4–7). The α, β, and δ isoforms are predominant in the kidney. Furthermore, the α and β isoforms are present in macrophages, T cells (8), and myofibroblasts (9), cell types that infiltrate the kidney in disease. Phosphorylation of p38α results in its translocation to the nucleus and the activation of transcription factors involved in production of proinflammatory mediators (10,11) and extracellular matrix proteins (12–14).

TGF-β1 is an important profibrotic mediator critical for collagen and matrix deposition (15), and TGF-β1 has been shown *in vitro* to be associated with the activation of p38α (16,17). Recent evidence has suggested that TGF-β1 activates the p38α and δ isoform of the p38 MAPK pathway via MKK3, and that TGF-β1–stimulated mesangial cells from MKK3-deficient mice had a reduction in pro–alpha I collagen expression compared with wild-type mice (18). In addition, p38 MAPK activation has been associated with production and secretion of TGF-β1 and extracellular matrix proteins (19). It is likely, therefore, that p38 MAPK activation has an important role in *in vivo* fibrosis independent of its proinflammatory effects, as both a downstream target of TGF-β1 signaling and an inducer of TGF-β1. In addition, connective tissue growth factor (CTGF), induced by TGF-β1 signaling, is an important mediator of collagen and tissue matrix protein production (20), but its relationship to p38 MAPK activation has not previously been studied.

p38 MAPK activation has been demonstrated in the lung of patients with pulmonary fibrosis (21). Blockade of p38 has been demonstrated to inhibit TGF-β1–induced collagen expression in fibroblasts, hepatic cells, and mesangial cells *in vitro* (22–24). In animal models of toxic inflammatory lung injury, blockade of p38 MAPK has been shown to reduce fibrosis (25,26). Fibrosis in these animal models is in part as a consequence of an initial inflammatory insult, and inhibition of tissue inflammation by p38 blockade may have contributed to a reduction in tissue fibrosis. Thus, direct evidence of a role for p38 MAPK activation in fibrosis *in vivo* is lacking.

Received June 20, 2003. Accepted October 31, 2003.

Correspondence to: Dr. Cosimo Stambe, Department of Nephrology, Monash Medical Centre, 246 Clayton Road, Clayton, Melbourne, Australia, 3168. Phone: 61-3-95943568; Fax: 61-3-9594-3650; E-mail: cosimo.stambe@med.monash.edu.au

1046-6673/1502-0370
Journal of the American Society of Nephrology

DOI: 10.1097/01.ASN.0000109669.23650.56

We thus examined activation of p38 MAPK in a model of renal fibrosis induced by a noninflammatory surgical insult, unilateral ureteric obstruction (UUO) and localized activation of the pathway to cells within obstructed kidney. With the use of a specific inhibitor of p38α, NPC 31169, we examined the contribution of p38α activation to the development of renal fibrosis.

Materials and Methods

Rat UUO

Renal fibrosis was induced by ligation of left ureter, UUO, in inbred female Sprague-Dawley rats (140 to 180 g, Monash Animal Services, Melbourne, Australia). Briefly, rats were anesthetized, laparotomy performed, and the left ureter identified and ligated at two points along the ureter 1 cm apart. Groups of six animals were killed at 6 h, 1 d, and 7 d after UUO. When killed, the kidneys were fixed for 4 h in 4% formalin for histopathology analysis. Animal experiments were approved by the Monash Medical Centre Animal Ethics Committee.

Antibodies

The following mouse monoclonal antibodies were used in this study: anti-phospho p38 (p-p38, Sigma-Aldrich, St. Louis, MO) raised against the dual phosphorylated tyrosine and threonine residues of the p38 peptide and recognizing all of the phosphorylated p38 isoforms; anti-p38α (anti-SAPK2a, Upstate, New York, NY), recognizing the nonphosphorylated and phosphorylated p38α isoform; ED1, anti-CD68 recognizing rat macrophages (Serotec, Oxford, UK); OX-1, anti-CD45 supernatant recognizing rat leukocytes; R73, recognizing rat lymphocytes; anti–α_1-tubulin (Sigma-Aldrich); 1A4, anti–alpha smooth muscle actin (α-sma, Sigma-Aldrich); anti-collagen IV (Dako, Glostrup, Denmark); and anti–heat shock protein 47 (Hsp47) recognizing rat collagen chaperone protein (Stressgene Biotechnologies, Victoria, Canada). The following rabbit polyclonal antibody was used: anti-TGF-β1 (Santa Cruz, Santa Cruz, CA). Horseradish peroxidase and alkaline phosphatase–conjugated goat anti-mouse IgG, and peroxidase-conjugated mouse anti-peroxidase complexes (PAP) were purchased from Dako.

Western Blot Analysis

At the time the animals were killed, the obstructed kidney from each animal was crushed and suspended in 1.0 ml of lysis buffer containing 10 mM Tris-HCl pH 7.4, 100 mmol NaCl, 1 mM EDTA, 1 mM EGTA, 1 mM NaF, 2 mM Na_3VO_4, 0.1% SDS, 1% Triton X-100, 0.5% deoxycholate, 1 mM phenylmethylsulfonyl fluoride, and 10% proteinase inhibitor (Sigma-Aldrich) and left on ice for 15 min, vortexing every 2 min. The samples were centrifuged at 14,000 rpm for 10 min and the supernatant stored at −80°C. Protein estimations were performed with a Bradford assay (Pierce, Rockford, IL). Protein was loaded at 100 μg per well and separated by SDS-PAGE on a 12.5% acrylamide gel. Gels were electroblotted onto a PVDF membrane, and the blots were incubated for 2 h in 20 ml of blocking buffer (50 mM Tris-HCl, 350 mM NaCl, 0.5% Tween20 with 5% skim milk). Blots were then washed three times in wash buffer (50 mM Tris-HCl, 350 mM NaCl, 0.02% Tween20 pH 7.5) and incubated with either anti-p38α (1 μg/ml) or anti–p-p38 (2 μg/ml) in 5% BSA in wash buffer overnight at 4°C. Blots were washed three times, then incubated with horseradish peroxidase conjugated goat anti-mouse IgG for 2 h at room temperature, washed three times, and the membrane-bound antibody detected by Supersignal West Pico chemiluminescent substrate (Pierce) and captured on x-ray film.

To determine the equivalence of protein loading, membranes were stripped with ×1 stripping buffer (Chemicon International, Temecula, CA), blocked with 20 ml of blocking buffer for 2 h, and then probed with anti–α_1-tubulin (1:2000) in 5% BSA in wash buffer overnight. Membranes were washed three times and incubated with horseradish peroxidase conjugated goat anti-mouse IgG, washed in wash buffer three times, and developed with chemiluminescence (Pierce) and captured on x-ray film. Densitometry analysis was performed by a Gel Pro analyser program (Media Cybernetics, Silver Spring, MD).

Immunohistochemistry

Slices of the obstructed kidney were fixed in 4% buffered formalin (for p-p38, CD68, 1A4, Hsp47, fibronectin, and TGF-β1 immunostaining) and embedded in paraffin. Four-micron sections were cut, dewaxed in histosol, and rehydrated. Alternatively, tissue was fixed in 2% paraformaldehyde-lysine-periodate for 3.5 h, snap-frozen in OCT, and 4-μm cryostat sections cut for p38α, CD45, T cell, and collagen IV immunostaining. Immunohistochemical staining was performed as described previously (27). Briefly, the sections were microwave oven–heated in a Dako microwave buffer for 10 min and allowed to cool. All sections were washed in PBS, blocked with 10% normal sheep serum plus 10% FCS in PBS for 30 min at room temperature, and incubated overnight at 4°C with anti–p-p38, anti-p38α, anti-CD68, anti-CD45, R73, 1A4, anti-collagen IV, anti-Hsp47, or anti–TGF-β1 in 10% normal rat serum, 1% BSA in PBS. Sections were subsequently washed once in PBS, endogenous peroxidase inactivated in 1% H_2O_2 in methanol for 20 min, incubated with horseradish peroxidase–conjugated goat anti-mouse (or rabbit) IgG followed by mouse (or rabbit) PAP, and developed with 3,3-diamenobenzidine to produce a brown color. We have previously demonstrated specificity of p-p38 immunostaining by using absorption of the p-p38 antibody with p-p38 or irrelevant phosphopeptides (28).

When double labeling, the sections were immunostained by means of the PAP method described above and then were microwave oven–heated, blocked with 10% normal sheep serum and 10% FCS in PBS, and incubated with 1A4 (1:2000) overnight at 4°C in 10% normal rat serum and 1% BSA, incubated with horseradish peroxidase–conjugated goat anti-mouse IgG followed by mouse PAP, and developed with Vector SG (Vector Laboratories, Burlingame, CA) to produce a gray color.

NPC 31169 Kinase Assays

NPC 31169 was developed by Scios Inc. (San Francisco, CA) and inhibits the active (phosphorylated) form of p38α MAPK. Specificity for p38α inhibition was determined in kinase assays. Individual kinases were isolated from cell lysates by immunoprecipitation. Kinase assays were performed as described previously (29). Briefly, kinases were incubated with their specific target substrates together with 0.1 mM [g^{32}P]ATP for 10 min at 30°C in the presence of increasing concentrations of NPC 31169. Protein was precipitated, washed in 50 mM phosphoric acid to remove ATP, and radioactivity counted. The concentration of NPC 31169 required to inhibit kinase activity by 50% was recorded as a 50% inhibitory concentration value (Table 1).

p38α MAPK Blockade in Rat UUO

Groups of eight animals were gavaged with NPC 31169 at 40 mg/kg in polyethylene glycol 400 or with vehicle alone 2 h before the ligation of the left ureter, and treatment continued as twice-daily gavages of NPC 31169 (40 mg/kg) or vehicle alone for 7 d. Animals

Table 1. Specificity of p38 inhibition by NPC 31169 *in vitro*

Kinase	IC_{50} (μM)[a]
p38α	0.0032
p38β	0.12
p38γ	>50
ERK2	>50
JNK1	>50
TGFβ-R1	>50
TGFβ-R2	>50
PKC	>50
PKA	>50
cdc2	>50
EGFR	>50
PKD	>50
MAPKAPK2	>50

[a] Concentrations of NPC 31169 (μM) resulting in a 50% reduction in the activity of kinase enzymes (IC_{50}) as determined by *in vitro* phosphorylation of their substrates.

were killed and blood and tissue collected. Serum creatinine measurements were performed by the Department of Biochemistry, Monash Medical Centre, with a Dupont ARL analyzer. Full blood counts were performed on a Cell-Dyn 3700 automated cell counter (Abbott Laboratories, Abbot Park, IL). Obstructed kidney was fixed for immunostaining, or total RNA extracted for Northern blot test by tissue lysis with TriZol (Life Technologies, Grand Island, NY) according to the manufacturer's instruction and stored at −80°C.

Quantification of Interstitial Volume, Leukocyte and Myofibroblast Accumulation, and Extracellular Matrix Deposition

All analyses were performed on blinded slides. Interstitial volume was assessed on 3-μm periodic acid–Schiff–stained formalin-fixed sections at ×250 magnification by counting the number of intersecting points that fall between tubules on a defined 100-point grid. Glomeruli and large vessels were excluded. A total of 10 fields per animal were counted and the results expressed as a percentage of the total number of grid points counted. Interstitial T cells and macrophages were scored by counting the number of immunostained cells per high-power field (×400) on 20 fields per animal and expressed as cells per square millimeter. α-sma, collagen IV, and TGF-β1 staining were assessed by image analysis of 20 fields (×250 magnification), excluding glomeruli, per animal (Image-Pro Plus Software, Media Cybernetics) and the results expressed as the percentage of the area of the cortex stained. Interstitial Hsp47 staining was scored by counting the number of intersecting points of a grid falling on positively stained interstitial cells on 4-μm formalin-fixed sections at ×250 magnification. A total of 20 fields per animal were counted and the results expressed as a percentage of the number of Hsp47-positive points per 1000 points counted. Glomeruli and large vessels were excluded.

Northern Blot Analysis

Probes used for Northern blot analysis were as follows. Rat α-sma, TGF-β1, and glyceraldehyde phosphate dehydrogenase (GAPDH) cDNA were cloned into pMOSBlueT-vector (Amersham, Buckinghamshire, England). Mouse collagen α1 (IV) and rat CTGF were cloned into pCRII-TOPO vector (InVitrogen, San Diego, CA). Except for GAPDH, anti-sense cRNA probes were labeled with digoxigenin (DIG)–UTP (Roche, Mannheim, Germany) by using either T7 RNA polymerase for pMOS-Blue T-vector or SP6 RNA polymerase for the cDNA inserts cloned into pCRII-TOPO vectors. The antisense GAPDH cRNA probe was labeled with fluorescein (FITC)–UTP (Roche) by using the T7 RNA polymerase.

Total RNA from normal and obstructed kidney was extracted with TriZol (InVitrogen) according to the manufacturer's instructions. A total of 15 μg of RNA was denatured with glyoxal and DMSO and size-fractionated on 1.2% agarose gels and capillary-blotted onto nylon membranes (Amersham). Membranes were hybridized in DIG Easy Hybridization Buffer (Roche) with either DIG-labeled RNA probes or FITC-labeled cRNA probes at 68°C. After hybridization, membranes were finally washed in 0.1× SSC/0.1% SDS at 68°C. Bound probes were detected by means of alkaline phosphatase conjugated sheep anti-DIG antibody (Fab) or sheep anti-FITC antibody and then incubated with CDP-Star (Roche) reagent and chemiluminescence captured on Kodak BMR film. Densitometry analysis was performed by the Gel Pro analyzer program (Media Cybernetics).

Statistical Analyses

Data are presented as mean ±1 SD. Comparisons were made between groups of animals by ANOVA by the Bonferroni correction for multiple comparisons (GraphPad Software, San Diego, CA).

Results

p38 MAPK Activation in Normal and Obstructed Kidney

In normal kidney, the tubules are tightly packed with few interstitial cells (Figure 1a). By Western blot test, p38α and p-p38 were present in whole kidney lysates of normal animals (Figure 2, a and b). Immunostaining demonstrated that p38α was localized to the luminal surface of many tubules in normal kidney (Figure 3a). In most tubules with luminal staining, nuclear staining for p38α was not seen, suggesting that p38α was not activated in these cells. Conversely, nuclear, but not luminal, p38α staining was seen in a few tubules. Taken together, these data suggest tubular activation and nuclear translocation of cytoplasmic p38α in a few tubules of normal rat kidney (Figure 3a). p-p38 was localized to the nuclei of some tubular cells in normal kidney, with variation in the intensity of staining (Figure 3e).

Unilateral ureteric ligation caused tubular dilation in the obstructed kidney, leading to the loss of tubular epithelial cells and an increase in interstitial volume and cellularity by day 7 (Figure 1b). Western blot test showed that the level of p38α protein was increased within 6 h of ureteric ligation compared with normal, and continued to increase up to day 7 of obstruction (Figure 2a). At 6 h UUO, there was a loss of p38α luminal staining within dilated tubules, with an increase in nuclear staining in these tubules (Figure 3b). This immunostaining pattern was more pronounced at day 7 UUO, in which luminal staining was absent in many tubules with increased nuclear staining (Figure 3c)

By Western blot test, there was an increase in p-p38 seen in the obstructed kidney compared with normal, being elevated at 6 h after UUO and increasing to 13-fold above normal by day 7 (Figure 2b). The number of p-p38–positive nuclei was in-

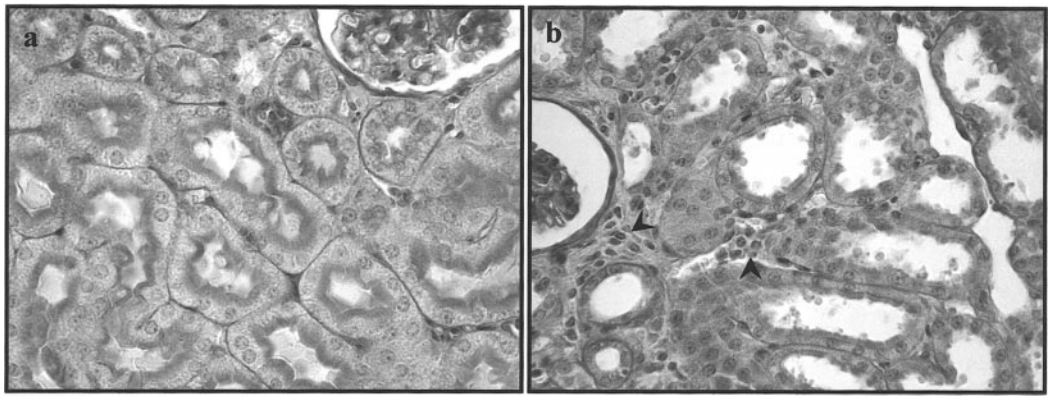

Figure 1. Periodic acid–Schiff (PAS) stain of normal and obstructed kidney. Normal kidney (a) and obstructed kidney 7 d after unilateral ureteric ligation (b) were stained with PAS and counterstained with hematoxylin. Tubules of normal kidney (a) were tightly packed, whereas tubules of obstructed kidney were dilated (b) and there is a significant interstitial infiltrate (b, arrowhead). Original magnification, ×400.

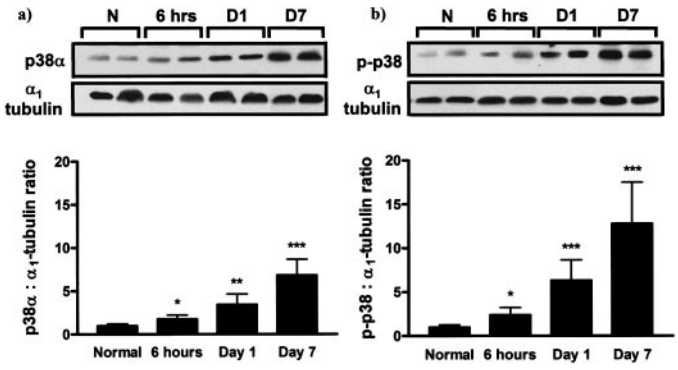

Figure 2. Increase in p38α and phosphorylated p38 (p-p38) in obstructed kidney. Whole kidney lysates from normal rat kidneys and obstructed kidneys from rats 6 h, 1 d, and 7 d after ureteric ligation were examined for the presence of p38α (a, b) and p-p38 (c, d) by Western blot analysis. Blots were stripped and probed for α_1-tubulin as a loading control. Two representative animals are shown at each time point. Graphs show densitometry analysis (mean ±1 SD, groups of six animals) of the ratio of p38α or p-p38 to α_1-tubulin compared with normal animals (assigned a p38α or p-p38 to α_1-tubulin ratio of 1; $*P < 0.05$, $**P < 0.01$, $***P < 0.001$ *versus* normal).

creased in dilated tubules at 6 h and day 7 UUO (Figure 3, f and g).

The obstructed kidney is characterized by an interstitial infiltrate of myofibroblasts, macrophages, and lymphocytes. Myofibroblasts detected by immunostaining for a cytoplasmic marker, α-sma, were positive for both p38α and p-p38 in a nuclear staining pattern (Figure 3, d and h). α-sma staining was restricted to interstitial cells and blood vessels (Figure 3, d and h). Serum creatinine estimations at the time of death were normal in drug- and vehicle-treated animals, suggesting that significant NPC 31169 nephrotoxicity in the normal nonobstructed contralateral kidney does not occur (51.5 ± 6.3 μmol/L in drug-treated animals *versus* 53.2 ± 7.1 μmol/L in vehicle-treated animals; $P = 0.23$). No toxicity in terms of body weight, condition of the animal, hemoglobin, white blood cell count, and platelet count was seen (data not shown).

p38α Blockade Reduces Interstitial Myofibroblast Accumulation and Renal Fibrosis

To assess the functional contribution of p38 MAPK activation to the development of interstitial fibrosis in UUO, we treated animals with a specific inhibitor of p38α, NPC 31169 (Table 1). Compared with vehicle-treated animals, NPC 31169 treatment reduced interstitial volume by 56% in rats at day 7 after UUO (Figure 4a). In addition, there was a 51% reduction in collagen IV mRNA expression in whole kidney with NPC 31169 treatment (Figure 5a) and a 29% (percentage of area stained) reduction in matrix collagen IV immunostaining compared with vehicle treatment (Figure 6, a–c). This reduction was not attributed to a reduction in infiltrating leukocytes because the number of interstitial macrophages and lymphocytes were not different in NPC 31169–treated animals compared with vehicle-treated animals (Figure 4b).

Infiltrating myofibroblasts at day 7 after ureteric ligation was reduced NPC 31169 treatment, as shown by a 61% reduction in α-sma mRNA expression in whole kidney by Northern blot test (Figure 5b) and a 44% reduction in interstitial α-sma immunostaining as determined by the percentage of area of cortex stained (Figure 6, d–f) compared with vehicle-treated animals. Collagen production and secretion by both myofibroblasts and tubular cells are associated with Hsp47 production. Interstitial Hsp47 may therefore be a useful marker of the number of myofibroblasts present. In animals treated with NPC 31169, interstitial Hsp47 immunostaining was reduced by 45% compared with vehicle-treated animals (point counting, Figure 6, g–i).

Upregulation of TGF-β1 Production in UUO Is Not Affected by p38α MAPK Blockade

To determine whether the reduction in renal fibrosis with p38α blockade was associated with an alteration in TGF-β1, we examined TGF-β1 protein production by immunostaining and TGF-β1 mRNA by Northern blot test. Immunohistochemistry of normal kidney shows weak TGF-β1 staining in a few cortical tubules (data not shown). In obstructed kidney, there was strong immunostaining of TGF-β1 in dilated and injured

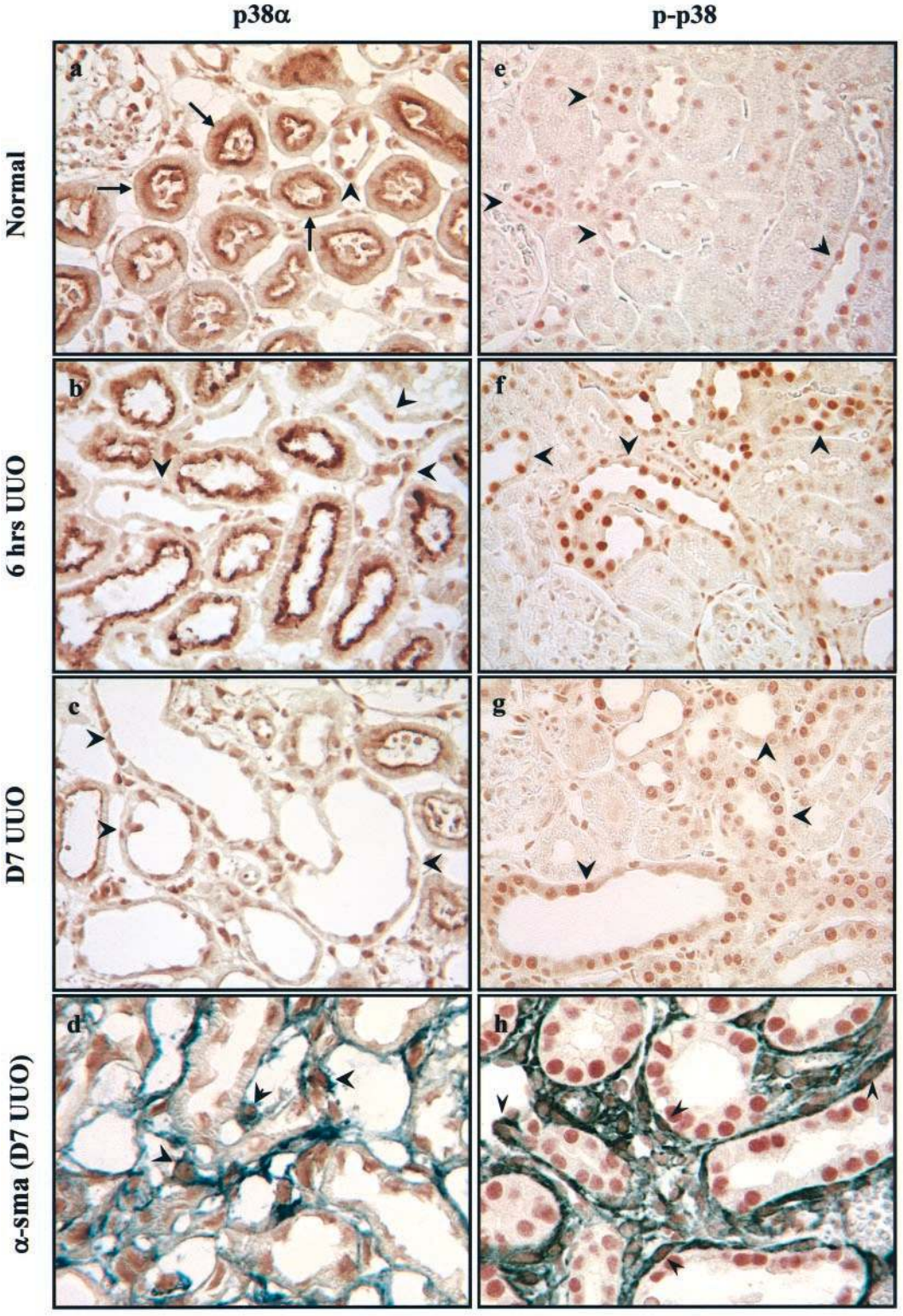

Figure 3. Immunolocalization of p38α and phosphorylated p38 (p-p38) in normal and obstructed kidney. In normal rat kidney, p38α (a, brown, arrows) was localized to the luminal surface of most tubules. Many of these tubules do not exhibit nuclear p38α localization. In some tubules, however, p38α was localized to the nucleus with no cytoplasmic staining evident (arrowhead). At 6 h after unilateral ureteric obstruction (UUO) p38α (b) was localized to the nucleus with a loss of luminal staining (arrowheads) in dilated and injured tubules. At day 7 after ureteric ligation, there was a further loss of p38α cytoplasmic staining with an increase in nuclear staining (c, arrowheads). At day 7 UUO, p38α (d, brown) was also localized to the nuclei of myofibroblasts (arrowheads), detected by immunostaining for a cytoplasmic marker of myofibroblasts, alpha–smooth muscle actin (α-sma, gray). In normal rat kidney, p-p38 (e, brown, arrowheads), was localized to the nuclei of some tubules. Nuclear p-p38 was increased in dilated tubules at 6 h (f), with a further increase at 7 d after ureteric ligation (g, arrowhead). At day 7 UUO, p-p38 (h, brown) was also localized to the nuclei of myofibroblasts (arrowheads), detected by immunostaining for alpha smooth muscle actin (α-sma; gray). Original magnification, $\times$800.

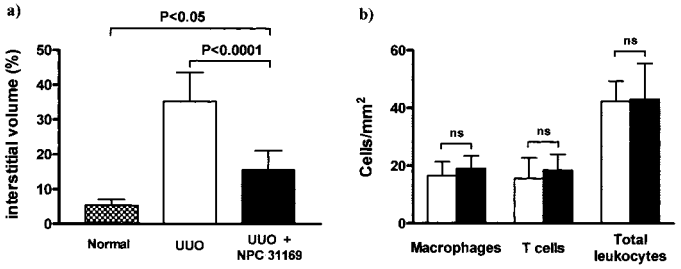

Figure 4. p38α mitogen-activated protein kinase (MAPK) blockade reduces interstitial volume in obstructed kidneys but does not reduce the number of infiltrating interstitial leukocytes. (a) Compared with normal kidneys (checkered bar), there was a dramatic increase in interstitial volume by point counting 7 d after ureteric ligation in animals treated with vehicle (open bar). This was reduced by p38α blockade with NPC 31169 treatment (solid bar). (b) NPC 31169 treatment (solid bar) did not reduce the number of interstitial macrophages, T cells, and total leukocytes in day 7 obstructed kidneys compared with vehicle treatment (open bar). Data are represented as the mean (±1 SD) of groups of eight animals.

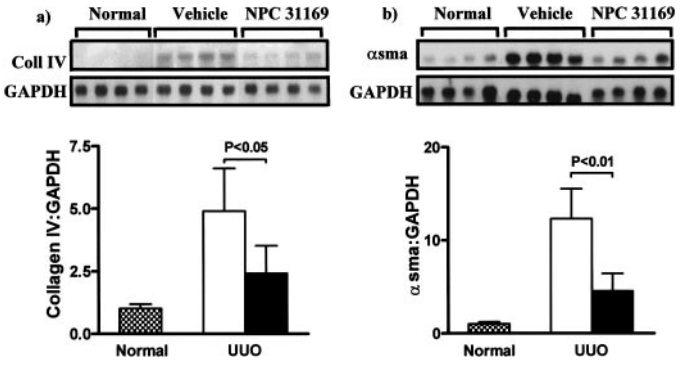

Figure 5. p38α mitogen-activated protein kinase (MAPK) blockade reduces collagen IV and alpha–smooth muscle actin (α-sma) mRNA expression in obstructed kidney. Compared with normal kidneys (checkered bar), there was a dramatic increase in (a) collagen IV and (b) α-sma mRNA expression by Northern blot test in obstructed kidneys of vehicle-treated (open bar) animals 7 d after ureteric ligation. p38α blockade with NPC 31169 treatment (solid bar) reduced collagen IV and α-sma mRNA expression in obstructed kidneys. Four representative animals are shown for each group. Graphs show densitometry analysis (mean ±1 SD, groups of eight animals) of the ratio of collagen IV and α-sma to glyceraldehyde phosphate dehydrogenase (GAPDH) compared with normal animals (assigned an α-sma or collagen IV to GAPDH ratio of 1).

tubules, and to a much smaller degree the interstitium. Compared with vehicle-treated animals, TGF-β1 immunostaining, as determined by the percentage of area of cortex stained, is unaltered with NPC 31169 treatment at day 7 obstruction (Figure 7, a–c). Northern blot analysis demonstrated an increase in TGF-β1 mRNA at day 7 obstruction, which was unaffected by NPC 31169 treatment (Figure 7d). In addition, we examined CTGF, a downstream target of TGF-β1 involved in extracellular matrix production. Compared with vehicle-treated animals, CTGF mRNA expression was reduced by 62% in NPC 31169–treated animals at day 7 UUO (Figure 7e).

Discussion

In the study presented here, we examined the role of p38 MAPK activation in renal fibrosis in a model of surgically induced tissue injury, rat UUO. We first established an increase in both p38α and activated p38 (p-p38) in obstructed kidney through a time course of UUO. By immunolocalization, we demonstrated a loss of luminal p38α with a concomitant increase in nuclear p38α and p-p38 within injured and dilated tubules. This staining pattern suggests that cytoplasmic p38α is activated by phosphorylation and translocates to the nucleus of the injured tubular cell during obstruction. In addition, we localized both p38α and p-p38 to nuclei of interstitial myofibroblasts—cell types central to the development of interstitial fibrosis in the obstructed kidney. With the use of a specific inhibitor of p38α, we demonstrated a functional role for p38α MAPK pathway activation in renal fibrosis, independent of TGF-β1 protein and mRNA levels, but with a reduction in CTGF mRNA expression.

The reduction in extracellular matrix deposition with p38 MAPK blockade in UUO was proportional to the reduction in interstitial myofibroblast accumulation, as demonstrated by a reduction in α-sma staining and mRNA expression. However, recent evidence has suggested that p38 may be involved in TGF-β1–induced α-sma production, and therefore, α-sma may not necessarily reflect the amount of tissue myofibroblast infiltration (30,31). To confirm our findings, we assessed interstitial Hsp47, a collagen chaperone protein produced by myofibroblasts during collagen production and independent of p38 activation. The amount of interstitial Hsp47 protein may therefore more accurately represent the number of interstitial myofibroblasts present. Compared with vehicle-treated animals, treatment with NPC 31169 showed a reduction in interstitial Hsp47 staining, consistent with the degree of reduction in interstitial α-sma–positive cell accumulation.

This reduction in interstitial myofibroblast accumulation may be as a result of inhibition of myofibroblast migration or a decrease in myofibroblast transdifferentiation of tubular and smooth muscle cells. Previous *in vitro* reports have demonstrated the importance of p38 MAPK activation to PDGF-BB mediated migration of hepatic myofibroblasts (32). Furthermore, TGF-β1 has been demonstrated to induce myofibroblast transdifferentiation of tubular cells both *in vitro* (33) and in UUO (34) and TGF-β1–induced mammary epithelial cell migration and subsequent fibroblast transdifferentiation is dependent on p38 MAPK activation (35). It is therefore possible that p38 MAPK inhibition in this study resulted in a reduction in interstitial myofibroblast accumulation by interfering with both TGF-β1 mediated myofibroblast and epithelial migration, and myofibroblast transdifferention of tubular cells and smooth muscle cells.

p38 MAPK activation occurred within tubules and infiltrating myofibroblasts of the obstructed kidney, and p38α MAPK blockade may have inhibited collagen production in this study via an effect on either or both of these cell types. *In vitro* studies have demonstrated TGF-β1–induced collagen expression in myoblasts via p38 MAPK activation (36). TGF-β1–

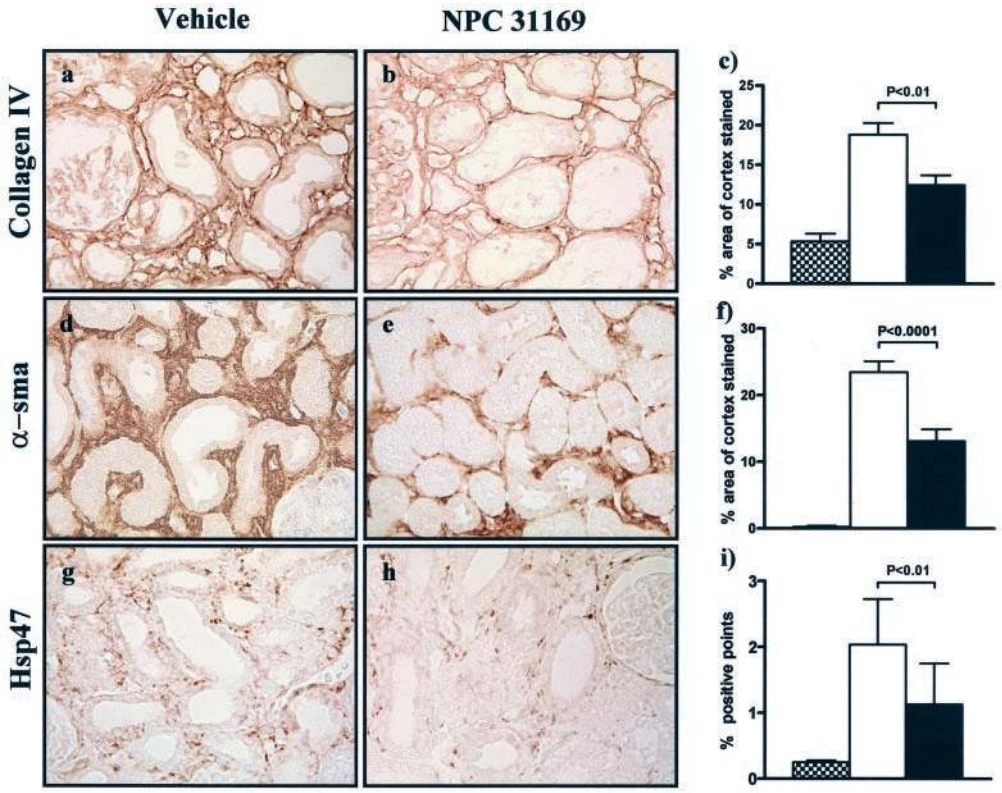

Figure 6. p38α mitogen-activated protein kinase (MAPK) blockade reduces collagen IV, alpha–smooth muscle actin (α-sma) and heat shock protein 47 (Hsp47) immunostaining in obstructed kidneys. Compared with vehicle treatment (open bar), obstructed kidneys of animals treated with NPC 31169 (solid bar) had a reduction in collagen IV (a–c, brown), interstitial myofibroblast accumulation (as determined by α-sma staining; d–f, brown), and Hsp47 (g–i, brown) at day 7 after ureteric ligation. Graphs show the analysis of the percentage of area of cortex stained for collagen IV and α-sma staining. For Hsp47 staining, the graph shows the number of Hsp47-positive interstitial points counted per 1000 points (expressed as a percentage). The data are represented as a mean ($\pm$1 SD) for groups of eight animals; normal kidney, checkered bar; vehicle-treated animals, open bar; NPC 31169–treated animals, solid bar. Original magnification, $\times$400.

induced extracellular matrix production by neonatal rat primary cardiac fibroblasts is inhibited by SB203055, an inhibitor of the p38 pathway (37), and activated mutants of MKK3 and MKK6, both upstream kinases of the p38 pathway, is associated with an increase in cardiac fibrosis (38). Proximal renal tubular cells are a known source of TGF-β1 and may promote peritubular myofibroblast collagen production and interstitial fibrosis (39). In addition, these cells may act as effectors for collagen IV production and deposition, an effect mediated by TGF-β1 (40).

Despite recent *in vitro* evidence of a role for p38 activation in TGF-β1 production (19), we were unable to demonstrate this *in vivo*. In our study, TGF-β1 mRNA expression and protein is increased in obstructed kidney and unaffected by p38 MAPK blockade. TGF-β1 was localized predominantly to the dilated and injured tubules of obstructed kidney. The inability to suppress TGF-β1 production by p38 blockade is consistent with recent studies demonstrating that angiotensin II–induced TGF-β1 production in vascular smooth muscle cells is mediated via the extracellular signal-related kinase MAPK and protein kinase C pathways (41,42).

CTGF is a downstream effector of TGF-β1 signaling and is important in the production of extracellular matrix proteins. It is localized to both tubular epithelial cells and the interstitium in UUO, and TGF-β1–induced fibronectin production is reduced with CTGF oligonucleotide antisense transfection of cultured renal fibroblasts (43). In this study, CTGF mRNA expression *in vivo* is reduced with p38α blockade and parallels the reduction in myofibroblast accumulation. From this study, it is not possible to discern whether the reduction in CTGF mRNA expression is as a consequence of the reduction in the number of interstitial myofibroblasts or whether there is a direct inhibitory effect on myofibroblast CTGF production with p38 blockade.

In UUO and other models of renal fibrosis, angiotensin II contributes to the development and progression of renal fibrosis by promoting the synthesis of growth factors and cytokines, including TGF-β1 (44) and TNF-α (45–47). TNF-α receptor I–deficient mice and pharmacologic inhibition of TNF-α receptor I partially reduces renal fibrosis in UUO (48). Furthermore, TNF-α is both a stimulus for p38 activation and is produced and secreted in response to p38 activation. The p38 MAPK is a common downstream target of TGF-β1 and TNF-α signaling in UUO, and blockade of p38 may therefore reduce interstitial fibrosis by inhibition of TGF-β1– and TNF-α–dependent extracellular matrix production.

UUO results in severe renal fibrosis as a consequence of a constant surgical insult. In this model, p38α blockade was

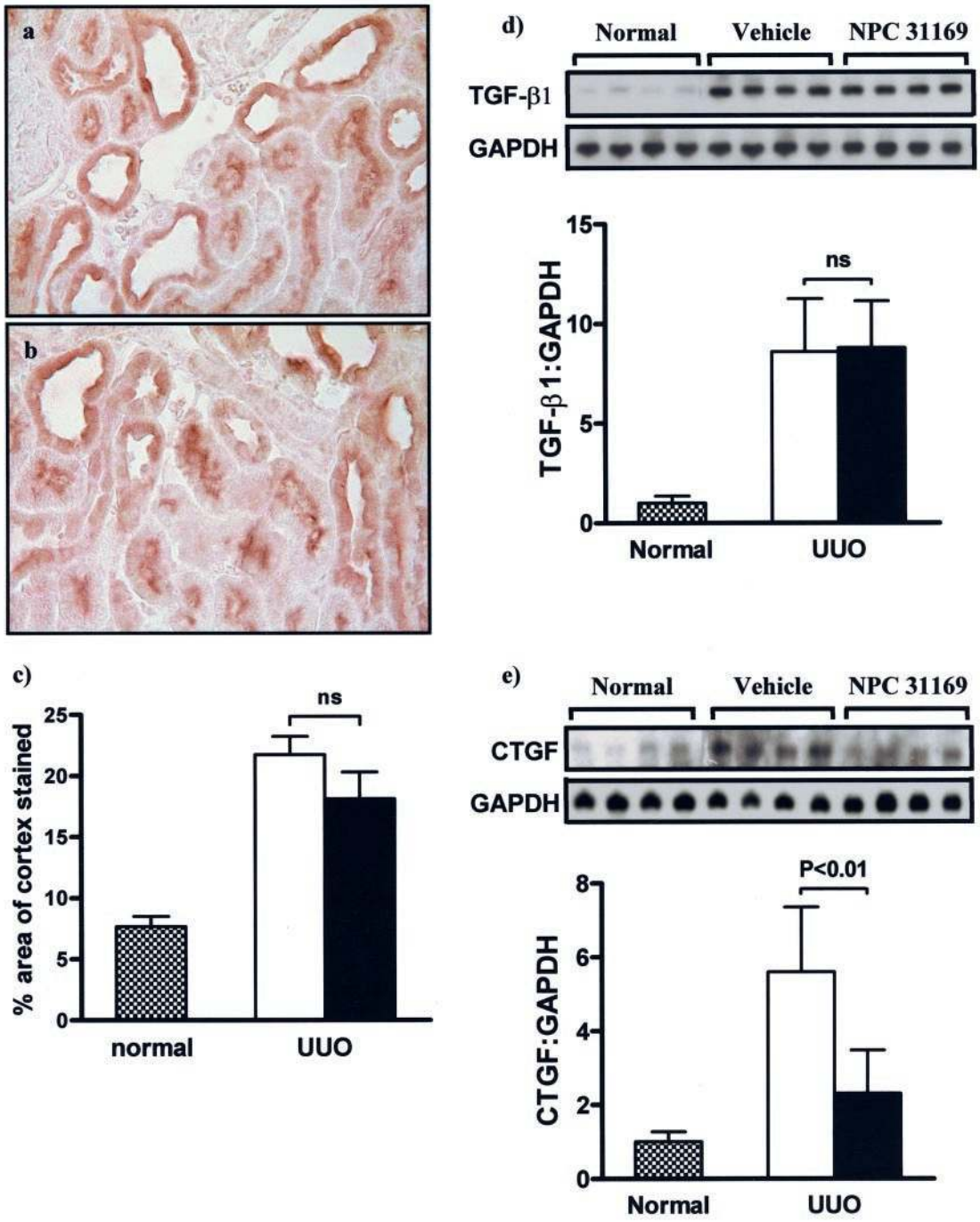

Figure 7. p38α mitogen-activated protein kinase (MAPK) blockade does not affect TGF-β1 immunostaining or mRNA expression in obstructed kidneys but does reduce CTGF mRNA expression. TGF-β1 immunostaining (a–c) and mRNA of TGF-β1 (d) and CTGF (e) by Northern blot test was examined in whole kidney 7 d after ureteric ligation. TGF-β1 (a, brown) was immunolocalized to dilated tubules of vehicle-treated animals 7 d after ureteric ligation and was unaffected by treatment with NPC 31169 (b, brown). TGF-β1 immunostaining was quantified as the percentage of area of cortex stained in normal animals (checkered bar), vehicle-treated animals (open bar), and NPC 31169–treated animals (solid bar) and the data expressed as the mean (±1 SD) for groups of eight animals. TGF-β1 mRNA expression (d) in 7 d obstructed kidneys of vehicle-treated animals (open bar) was increased compared with normal kidneys (checkered bar). This was unaffected by NPC 31169 treatment (solid bar). Four representative animals are shown for each group. Detection of glyceraldehyde phosphate dehydrogenase (GAPDH) was used as a loading control. Graph shows densitometry analysis (mean ± 1 SD, groups of eight animals) of the ratio of TGF-β1 to GAPDH compared with normal animals (assigned a TGF-β1 to GAPDH ratio of 1). CTGF mRNA expression (e) in 7-d obstructed kidneys of vehicle-treated animals (open bar) was reduced by NPC 31169 treatment (solid bar). Four representative animals are shown for each group. Detection of GAPDH was used as a loading control. Graph shows densitometry analysis (mean ±1 SD, groups of eight animals) of the ratio of CTGF to GAPDH compared with normal animals (assigned a CTGF to GAPDH ratio of 1).

associated with a significant reduction in fibrosis despite the presence of persistent stimulus for extracellular matrix production, ureteric ligation. Furthermore, increased TGF-β1 mRNA expression or protein production in UUO was not reduced after p38 blockade, suggesting that p38 activation mediates fibrosis downstream or independent of TGF-β1.

Two recent studies have demonstrated a reduction in bleomycin-induced pulmonary fibrosis with p38 inhibitors (25,26). Fibrosis after bleomycin is dependent on leukocyte mediated pulmonary injury (49,50). Thus, these studies cannot determine whether p38 blockade inhibited lung fibrosis through an action on leukocytes or through direct action on the myofibroblasts. We have demonstrated a reduction in fibrosis in a model of surgically mediated renal injury, consistent with a recent report demonstrating a reduction in cardiac fibrosis by using a transgenic approach to inhibit the p38α MAPK pathway in a non-inflammatory, pressure-overload model of cardiac hypertrophy and fibrosis (51).

In summary, we have identified a direct functional role for p38 MAPK activation in progressive renal fibrosis. p38α and p-p38 were increased in obstructed kidney, and we localized p38 MAPK activation to dilated and injured tubules, and infiltrating myofibroblasts. With the use of a novel and selective inhibitor of p38α, we were able to inhibit interstitial myofibroblast accumulation, reduce collagen IV mRNA expression and protein deposition, and reduce CTGF mRNA expression in spite of a continued increase in TGF-β1 mRNA expression and protein production. Therefore, p38α MAPK blockade may be a therapeutic option for the treatment of renal fibrosis.

Acknowledgment

This research was supported by grants from the National Health and Medical Research Council of Australia.

References

1. Lee JC, Laydon JT, McDonnell PC, Gallagher TF, Kumar S, Green D, McNulty D, Blumenthal MJ, Heys JR, Landvatter SW, Strickler JE, McLaughlin MM, Siemens IR, Fisher SM, Livi GP, White JR, Adams JL, Young PR: A protein kinase involved in the regulation of inflammatory cytokine biosynthesis. *Nature* 372: 739–746, 1994
2. Raingeaud J, Gupta S, Rogers JS, Dickens M, Han J, Ulevitch RJ, Davis RJ: Pro-inflammatory cytokines and environmental stress cause p38 mitogen-activated protein kinase activation by dual phosphorylation on tyrosine and threonine. *J Biol Chem* 270: 7420–7426, 1995
3. Ono K, Han J: The p38 signal transduction pathway: Activation and function. *Cell Signal* 12: 1–13, 2000
4. Wang XS, Diener K, Manthey CL, Wang S, Rosenzweig B, Bray J, Delaney J, Cole CN, Chan-Hui PY, Mantlo N, Lichenstein HS, Zukowski M, Yao Z: Molecular cloning and characterization of a novel p38 mitogen-activated protein kinase. *J Biol Chem* 272: 23668–23674, 1997
5. Jiang Y, Chen C, Li Z, Guo W, Gegner JA, Lin S, Han J: Characterization of the structure and function of a new mitogen-activated protein kinase (p38beta). *J Biol Chem* 271: 17920–17926, 1996
6. Jiang Y, Gram H, Zhao M, New L, Gu J, Feng L, Di Padova F, Ulevitch RJ, Han J: Characterization of the structure and function of the fourth member of p38 group mitogen-activated protein kinases, p38delta. *J Biol Chem* 272: 30122–30128, 1997
7. Li Z, Jiang Y, Ulevitch RJ, Han J: The primary structure of p38 gamma: A new member of p38 group of MAP kinases. *Biochem Biophys Res Commun* 228: 334–340, 1996
8. Hale KK, Trollinger D, Rihanek M, Manthey CL: Differential expression and activation of p38 mitogen-activated protein kinase alpha, beta, gamma, and delta in inflammatory cell lineages. *J Immunol* 162: 4246–4252, 1999
9. Wang YZ, Zhang P, Rice AB, Bonner JC: Regulation of interleukin-1beta–induced platelet-derived growth factor receptor-alpha expression in rat pulmonary myofibroblasts by p38 mitogen-activated protein kinase. *J Biol Chem* 275: 22550–22557, 2000
10. Waas WF, Lo HH, Dalby KN: The kinetic mechanism of the dual phosphorylation of the ATF2 transcription factor by p38 mitogen-activated protein (MAP) kinase alpha: Implications for signal/response profiles of MAP kinase pathways. *J Biol Chem* 276: 5676–5684, 2001
11. Rawadi G, Ramez V, Lemercier B, Roman-Roman S: Activation of mitogen-activated protein kinase pathways by *Mycoplasma fermentans* membrane lipoproteins in murine macrophages: Involvement in cytokine synthesis. *J Immunol* 160: 1330–1339, 1998
12. Ivaska J, Reunanen H, Westermarck J, Koivisto L, Kahari VM, Heino J: Integrin alpha2beta1 mediates isoform-specific activation of p38 and upregulation of collagen gene transcription by a mechanism involving the alpha2 cytoplasmic tail. *J Cell Biol* 147: 401–416, 1999
13. Reddy MA, Adler SG, Kim YS, Lanting L, Rossi J, Kang SW, Nadler JL, Shahed A, Natarajan R: Interaction of MAPK and 12-lipoxygenase pathways in growth and matrix protein expression in mesangial cells. *Am J Physiol Renal Physiol* 283: F985–F994, 2002
14. Kucich U, Rosenbloom JC, Shen G, Abrams WR, Hamilton AD, Sebti SM, Rosenbloom J: TGF-beta1 stimulation of fibronectin transcription in cultured human lung fibroblasts requires active geranylgeranyl transferase I, phosphatidylcholine-specific phospholipase C, protein kinase C-delta, and p38, but not erk1/erk2. *Arch Biochem Biophys* 374: 313–324, 2000
15. Sime PJ, O'Reilly KM: Fibrosis of the lung and other tissues: New concepts in pathogenesis and treatment. *Clin Immunol* 99: 308–319, 2001
16. Ge B, Gram H, Di Padova F, Huang B, New L, Ulevitch RJ, Luo Y, Han J: MAPKK-independent activation of p38alpha mediated by TAB1-dependent autophosphorylation of p38alpha. *Science* 295: 1291–1294, 2002
17. Hanafusa H, Ninomiya-Tsuji J, Masuyama N, Nishita M, Fujisawa J, Shibuya H, Matsumoto K, Nishida E: Involvement of the p38 mitogen-activated protein kinase pathway in transforming growth factor-beta–induced gene expression. *J Biol Chem* 274: 27161–27167, 1999
18. Wang L, Ma R, Flavell RA and Choi ME: Requirement of mitogen actived protein kinase kinase 3 (MKK3) for activation of p38alpha and p38delta MAPK isoforms by TGF-beta 1 in murine mesangial cells. *J Biol Chem,* 277: 47257–47262, 2002
19. Gruden G, Zonca S, Hayward A, Thomas S, Maestrini S, Gnudi L, Viberti GC: Mechanical stretch-induced fibronectin and transforming growth factor-beta1 production in human mesangial cells is p38 mitogen-activated protein kinase-dependent. *Diabetes* 49: 655–661, 2000
20. Leask A, Holmes A, Abraham DJ: Connective tissue growth factor: A new and important player in the pathogenesis of fibrosis. *Curr Rheumatol Rep* 4: 136–142, 2002

21. Yoshida K, Kuwano K, Hagimoto N, Watanabe K, Matsuba T, Fujita M, Inoshima I, Hara N: MAP kinase activation and apoptosis in lung tissues from patients with idiopathic pulmonary fibrosis. *J Pathol* 198: 388–396, 2002
22. Varela-Rey M, Montiel-Duarte C, Oses-Prieto JA, Lopez-Zabalza MJ, Jaffrezou JP, Rojkind M, Iraburu MJ: p38 MAPK mediates the regulation of alpha1(I) procollagen mRNA levels by TNF-alpha and TGF-beta in a cell line of rat hepatic stellate cells(1). *FEBS Lett* 528: 133–138, 2002
23. Sato M, Shegogue D, Gore EA, Smith EA, McDermott PJ, Trojanowska M: Role of p38 MAPK in transforming growth factor beta stimulation of collagen production by scleroderma and healthy dermal fibroblasts. *J Invest Dermatol* 118: 704–711, 2002
24. Chin BY, Mohsenin A, Li SX, Choi AM, Choi ME: Stimulation of pro-alpha(1)(I) collagen by TGF-beta(1) in mesangial cells: Role of the p38 MAPK pathway. *Am J Physiol Renal Physiol* 280: F495–504, 2001
25. Underwood DC, Osborn RR, Bochnowicz S, Webb EF, Rieman DJ, Lee JC, Romanic AM, Adams JL, Hay DW, Griswold DE: SB 239063, a p38 MAPK inhibitor, reduces neutrophilia, inflammatory cytokines, MMP-9, and fibrosis in lung. *Am J Physiol Lung Cell Mol Physiol* 279: L895–L902, 2000
26. Matsuoka H, Arai T, Mori M, Goya S, Kida H, Morishita H, Fujiwara H, Tachibana I, Osaki T, Hayashi S: A p38 MAPK inhibitor, FR-167653, ameliorates murine bleomycin-induced pulmonary fibrosis. *Am J Physiol Lung Cell Mol Physiol* 283: L103–L112, 2002
27. Lan HY, Mu W, Nikolic-Paterson DJ, Atkins RC: A novel, simple, reliable, and sensitive method for multiple immunoenzyme staining: Use of microwave oven heating to block antibody crossreactivity and retrieve antigens. *J Histochem Cytochem* 43: 97–102, 1995
28. Stambe C, Atkins RC, Tesch GH, Kapoun AM, Hill PA, Schreiner GF, Nikolic-Paterson DJ: Blockade of p38alpha MAPK ameliorates acute inflammatory renal injury in rat anti-GBM glomerulonephritis. *J Am Soc Nephrol* 14: 338–351, 2003
29. Davies SP, Reddy H, Caivano M, Cohen P: Specificity and mechanism of action of some commonly used protein kinase inhibitors. *Biochem J* 351: 95–105, 2000
30. Masamune A, Satoh M, Kikuta K, Sakai Y, Satoh A, Shimosegawa T: Inhibition of p38 mitogen-activated protein kinase blocks activation of rat pancreatic stellate cells. *J Pharmacol Exp Ther* 304: 8–14, 2003
31. Reeves HL, Dack CL, Peak M, Burt AD, Day CP: Stress-activated protein kinases in the activation of rat hepatic stellate cells in culture. *J Hepatol* 32: 465–472, 2000
32. Tangkijvanich P, Santiskulvong C, Melton AC, Rozengurt E, Yee HF Jr: p38 MAP kinase mediates platelet-derived growth factor-stimulated migration of hepatic myofibroblasts. *J Cell Physiol* 191: 351–361, 2002
33. Fan JM, Ng YY, Hill PA, Nikolic-Paterson DJ, Mu W, Atkins RC, Lan HY: Transforming growth factor-beta regulates tubular epithelial-myofibroblast transdifferentiation in vitro. *Kidney Int* 56: 1455–1467, 1999
34. Iwano M, Plieth D, Danoff TM, Xue C, Okada H, Neilson EG: Evidence that fibroblasts derive from epithelium during tissue fibrosis. *J Clin Invest* 110: 341–350, 2002
35. Bakin AV, Rinehart C, Tomlinson AK, Arteaga CL: p38 mitogen-activated protein kinase is required for TGFbeta-mediated fibroblastic transdifferentiation and cell migration. *J Cell Sci* 115: 3193–3206, 2002
36. Rodriguez-Barbero A, Obreo J, Yuste L, Montero JC, Rodriguez-Pena A, Pandiella A, Bernabeu C, Lopez-Novoa JM: Transforming growth factor-beta1 induces collagen synthesis and accumulation via p38 mitogen-activated protein kinase (MAPK) pathway in cultured L(6)E(9) myoblasts. *FEBS Lett* 513: 282–288, 2002
37. Akiyama-Uchida Y, Ashizawa N, Ohtsuru A, Seto S, Tsukazaki T, Kikuchi H, Yamashita S, Yano K: Norepinephrine enhances fibrosis mediated by TGF-beta in cardiac fibroblasts. *Hypertension* 40: 148–154, 2002
38. Liao P, Georgakopoulos D, Kovacs A, Zheng M, Lerner D, Pu H, Saffitz J, Chien K, Xiao RP, Kass DA, Wang Y: The in vivo role of p38 MAP kinases in cardiac remodeling and restrictive cardiomyopathy. *Proc Natl Acad Sci U S A* 98: 12283–12288, 2001
39. Abbate M, Zoja C, Rottoli D, Corna D, Tomasoni S, Remuzzi G: Proximal tubular cells promote fibrogenesis by TGF-beta1–mediated induction of peritubular myofibroblasts. *Kidney Int* 61: 2066–2077, 2002
40. Grande JP, Warner GM, Walker HJ, Yusufi AN, Cheng J, Gray CE, Kopp JB, Nath KA: TGF-beta1 is an autocrine mediator of renal tubular epithelial cell growth and collagen IV production. *Exp Biol Med (Maywood)* 227: 171–181, 2002
41. Hamaguchi A, Kim S, Izumi Y, Zhan Y, Yamanaka S, Iwao H: Contribution of extracellular signal-regulated kinase to angiotensin II–induced transforming growth factor-beta1 expression in vascular smooth muscle cells. *Hypertension* 34: 126–131, 1999
42. Gibbons GH, Pratt RE, Dzau VJ: Vascular smooth muscle cell hypertrophy vs. hyperplasia: Autocrine transforming growth factor-beta 1 expression determines growth response to angiotensin II. *J Clin Invest* 90: 456–461, 1992
43. Yokoi H, Mukoyama M, Sugawara A, Mori K, Nagae T, Makino H, Suganami T, Yahata K, Fujinaga Y, Tanaka I, Nakao K: Role of connective tissue growth factor in fibronectin expression and tubulointerstitial fibrosis. *Am J Physiol Renal Physiol* 282: F933–F942, 2002
44. Kaneto H, Morrissey J, Klahr S: Increased expression of TGF-beta 1 mRNA in the obstructed kidney of rats with unilateral ureteral ligation. *Kidney Int* 44: 313–321, 1993
45. Klahr S, Morrissey JJ: The role of vasoactive compounds, growth factors and cytokines in the progression of renal disease. *Kidney Int Suppl* 75: S7–S14, 2000
46. Hisada Y, Sugaya T, Yamanouchi M, Uchida H, Fujimura H, Sakurai H, Fukamizu A, Murakami K: Angiotensin II plays a pathogenic role in immune-mediated renal injury in mice. *J Clin Invest* 103: 627–635, 1999
47. Klahr S, Morrissey J: Angiotensin II and gene expression in the kidney. *Am J Kidney Dis* 31: 171–176, 1998
48. Guo G, Morrissey J, McCracken R, Tolley T, Liapis H, Klahr S: Contributions of angiotensin II and tumor necrosis factor-alpha to the development of renal fibrosis. *Am J Physiol Renal Physiol* 280: F777–F785, 2001
49. Izbicki G, Segel MJ, Christensen TG, Conner MW, Breuer R: Time course of bleomycin-induced lung fibrosis. *Int J Exp Pathol* 83: 111–119, 2002
50. Okazaki T, Nakao A, Nakano H, Takahashi F, Takahashi K, Shimozato O, Takeda K, Yagita H, Okumura K: Impairment of bleomycin-induced lung fibrosis in CD28-deficient mice. *J Immunol* 167: 1977–1981, 2001
51. Zhang S, Weinheimer C, Courtois M, Kovacs A, Zhang CE, Cheng AM, Wang Y, Muslin AJ: The role of the Grb2-p38 MAPK signaling pathway in cardiac hypertrophy and fibrosis. *J Clin Invest* 111: 833–841, 2003